RADIATION STABILITY OF COATINGS BASED ON TiO_2, ZnO AND SiO_2 NANOSTRUCTURED PIGMENTS TO PROTON EXPOSURE

Vitalii Neshchimenko[(1),(2)], Chundong Li[(2)], Mikhail Mikhailov[(2)]

[((1)]Science and Technology Materials Performance Evaluating in Space Environment Laboratory, Harbin Institute of Technology, Harbin, 150001, China, email: lichundong@hit.edu.cn, v1ta1y@mail.ru
[(2)] Radiation and Space Materials Laboratory, Tomsk State University of Control Systems and Radioelectronics, Tomsk, 634050, Russia, email: membrana2010@mail.ru

ABSTRACT

The effect of protons (E = 100 keV, F = $5x10^{15}$ cm^{-2}) exposure on the diffuse reflectance spectra of the coatings based on the TiO_2, ZnO and SiO_2 microsphere pigments in wavelength range from 250 to 2500 nm have been investigated. Evaluating the changes of the solar absorptance it was found that the radiation stability of the SiO_2 sphere particles coatings is higher than the radiation stability of TiO_2 and ZnO hollow particles coatings as well as the standard coatings based on this micropowders. The low radiation stability of the SiO_2 sphere particles is due to low radiation losses, low concentration of radiation-induced defects cause by presence of amorphous phase.

1 INTRODUCTION

The impact of the space environment on spacecraft leads to changes in properties and performance of the external materials, especially to increase in solar absorptance of thermal control coatings (TCC). The impact of space radiation is affected to spacecraft passing through all types of orbits from LEO to GSO. To a great extent it concerns white TCC of the class "solar reflectors", which include ceramic and enamel coating based on white pigments, polymer, and inorganic bonding agents [1].

The powders of SiO_2, TiO_2, ZnO had the widest application among the pigments for coatings of this class due to their high stability to impact of charged particles and solar ultraviolet radiation. However, a number of defects and absorption centers are formed in these pigments during a long-term spacecraft flight, which is enough to decrease the spectral reflectance in the ultraviolet (UV), visible and near-infrared (NIR) regions of the spectrum, and increase the solar absorptance (α_s) [2]. Therefore, the development of ways to increase radiation stability of coatings based on titanium dioxide is an urgent problem.

One innovating technique to improve the photo- and radiation-stability of coatings is to use microspheres as pigments, which are hollow particles with a high specific surface area. In such structures, radiation defects in bulk are less, as well as the surface defects being recombined on the thinner layer of the microspheres.

It is known that in conventional coatings based on polycrystalline oxides as pigments currently in use (Fig.1.(a)), the primary radiation defects produced from proton and electron exposure with energy below 300 keV are formed in layers approximately 5 μm, but secondary and thermalized defects may extend into deeper layers of the coating [3]. The color centers formed in polycrystals by radiation primarily impact on the optical properties of the coating, specifically on the reflectance and absorptance that are determined by a thickness of 80 μm.

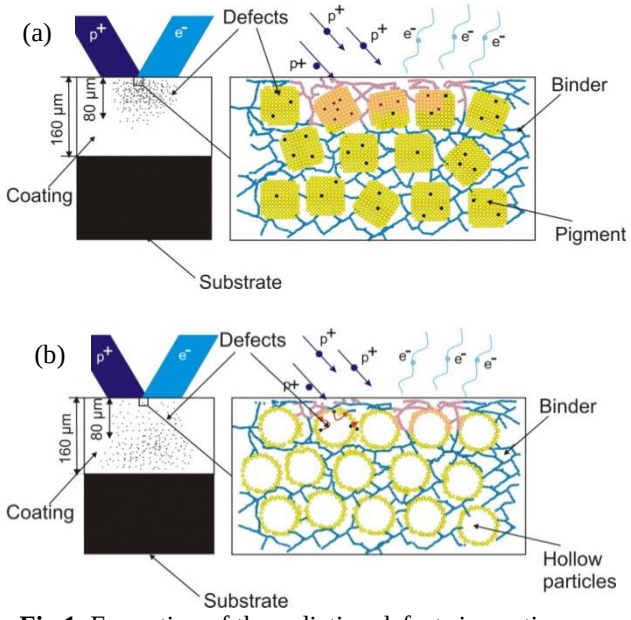

Fig.1. Formation of the radiation defects in coatings based on microparticles and hollow particles. [4]

One prospective new technology to improve the photo- and radiation-stability of coatings is to use microspheres as pigments, which are hollow particles with a high specific surface area. In such structures, radiation defects in bulk are less, as well as the surface defects being recombined on the thinner layer of the microspheres (Fig.1.(b)). The major portion of ions in ionizing radiation results in the creation of the defects in the depth of coatings (over 100 μm), due to the low ionization losses in the hollow particles. Thus, the defects formed in the depth of the material have the least effect on the optical properties of the coating. Also

nanostructured materials such as microspheres have low weight and low thermal conductivity compared with the pigment-polycrystalline that decreases the overall weight of a spacecraft.
This paper is devoted to the analysis of the reflective spectra of SiO_2, TiO_2, ZnO hollow particles and coatings based on them in the region of 200-2500 nm before and after irradiation by protons, and comparison of the obtained regularities with the data of coatings based on micropowders.

2 EXPERIMENTAL

The TiO_2, ZnO and SiO_2 micropowders with 99.8 % purity were purchased from Aladdin Chemistry Co. The synthesis of the TiO_2 and ZnO microsphere was carried out by the hydrothermal method [5], but SiO_2 by the formation of silica shells and dissolution of the polystyrene core particles.
Synthesis of hollow TiO_2 particles was carried out as in in the molar proportions $1(Ti(OCH(CH_3)_2)_4):12((C_4H_9)_4NOH):43(H_2O):170(C_2H_5OH)$ [6]. Titanium isopropoxide ($Ti(OCH(CH_3)_2)_4$) dissolved in ethanol and water, then in the resulting solution was added tetrabutylammonium hydroxide ($(C_4H_9)_4NOH$) and stirred on a magnetic stirrer for 30 minutes. The resulting solution was poured into an autoclave with Teflon cup which was heated at temperatures 200 ^oC during 6 hours. To increase the yield of separated spheres the γ-methacryloxypropyltrimethoxysilane were added to the solution. In the output the solution with a white precipitate was obtained which was washed several times with ethanol. The centrifugation was not performed, the powder precipitate itself, which was dried at 80 ^oC at air.
Hollow particles were obtained by hydrothermal method [7]: 2.5 mmol $Zn(CH_3COO)_2 \cdot 2H_2O$ was dissolved in 1 mol deionized water, after which 7.5 mmol NH_4HCO_3 was added. The solution was poured into a Teflon-lined autoclave, which was filled to 80 %. The sealed autoclave was maintained at 180 ^oC during 15 hours. After natural cooling the autoclave was opened, the white product were collected and sequentially washed several times by deionized water and ethanol. The centrifugation was not performed, the powder precipitate itself. Finally, the thick solution was dried in air at 60 ^oC with followed heat treatment at 650 ^oC during 3 hours.
Hollow SiO_2 particles were obtained by depositing Si (OC_2H_5) on solid substrates in the form of polystyrene beads in a solution of alcohol and ammonia water, followed by heat treatment at 600 ° C for 3 hours [8].
The coatings were prepared by mixing the powders with 50 % of volume and binder with 50 % of volume. The binder was a modified silicone varnish (methyl and methoxy group containing polysiloxane), with small additives of epoxy resin and some amount of hardener and stabilizers. The paint was coated with thickness 150-200 μm on the aluminum substrate 17 mm in diameter. The coating was sprayed by the airless method, which was obtained by dispersing the flow of the paint material.
Samples were tested using the Space Environment Simulator. The samples were irradiated by protons with energy of 100 keV fluence 5×10^{15} cm^{-2} with the flux 5×10^{11} $cm^{-2}s^{-1}$ in vacuum 2.5×10^{-4} Pa, while the initial vacuum was 5×10^{-5} Pa. Irregularity of the proton beam on the area sample did not exceed 5 %. During irradiation samples were maintained at 300 ± 5 K temperature.
The surface morphology of the hollow particles was analyzed by the scanning electron microscope (SEM) Helios NanoLab 600i and ZEISS EVO18. The specific surface area of the powder is determined by Brunauer-Emmet-Teller (BET) method with physical adsorption of nitrogen using AutoSorb 6iSA technique. The X-ray diffraction (XRD) analysis was carried out on a diffractometer Philips X'Pert PRO MRD (V = 40 kV, I = 40 mA, CuKα = 1.5405). The reflective spectra of the samples were measured using a Perkin Elmer Lambda 950 spectrophotometer with a scanning rate of 5 nm/s and a wavelength range from 250 to 2500 nm. The value of solar absorptance of the samples was calculated in accordance with ASTM (E490 and E903-00a-96).

3 RESULTS

From the micrographs obtained by the scanning electron microscope (Fig. 2) showed that during the reaction TiO_2, SiO_2, ZnO particles with a spherical shape 1-10 μm in average size are formed. The yield of hollow particles is about 90 %, other particles are bonded together or are the fragments of the spheres.
The specific surface area (SSA) of the synthesized particles measured by BET are presented in the table 1, measurements were carried out for two powders synthesized in different experimental series. The highest SSA value among microspheres is typical for TiO_2, but a high SSA value for the microcrystal is for ZnO.

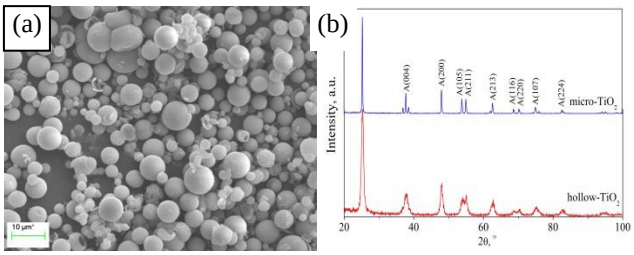

Fig.2. SEM images (a) and XRD patterns (b) of TiO_2 microspheres.

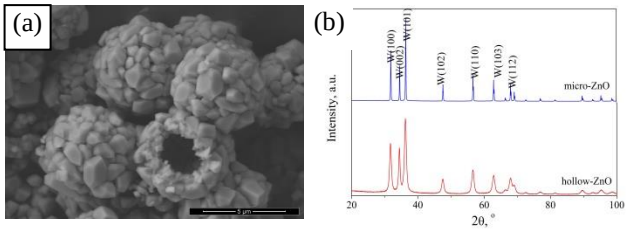

Fig.3. SEM images (a) and XRD patterns (b) of ZnO microspheres.

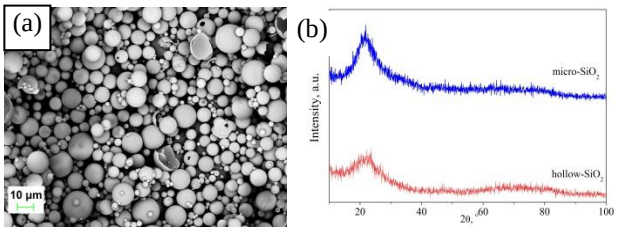

Fig.4. SEM images (a) and XRD patterns (b) of SiO_2 microspheres.

Table 1. Characterization of powders by average size distribution and specific surface area.

Type particles	Average size distribution, nm	Specific surface area, m^2/g
microcrystal-ZnO	700-1100	5.6 ± 1.8
microsphere-ZnO	4000-6000	32.8 ± 4.8
microcrystal-SiO_2	2000-5000	3.7 ± 1.1
microsphere-SiO_2	2000-10000	24.7 ± 6.2
microcrystal-TiO_2	800-1000	4.3 ± 1.3
microsphere-TiO_2	2000-5000	41.2 ± 5.4

X-ray diffraction analysis showed (Fig. 2b) that the synthesized hollow TiO_2 particles have peaks related to the anatase structure (*I41/amd*), there are no amorphous phases. The parameters of the unit cell for hollow particle are: $a = 3.873 \pm 0.003$, $c = 10.50 \pm 0.008$ Å. For microparticles it is equal: $a = 3.799 \pm 0.002$ Å, $c = 9.756 \pm 0.003$ Å. Such changes of constant lattice are associated with various tensile stresses caused by packing defects and leading to inelastic deformation of the grating. For hollow particles such distortions occur along the *c* axis, for nanoparticles tensile stresses act along the *a* axis.

Changes in the lattice constants occur also in nano- and hollow particles of zinc oxide (рис.3.b). The structural type of these powders is wurtzite (*P63mc*). The constants of the crystal lattice of the microparticles were: $a = 3.249 \pm 0.003$ Å, $c = 5.205 \pm 0.004$ Å. For nanoparticles, it has been established that the parameters *a* and *c* increase to 3.2549 ± 0.002 Å and 5.2104 ± 0.003 Å, respectively. Values of lattice parameters *a* and *c* for hollow particles are in the range between the values for micro- and nanoparticles.

It follows from the XRD patterns that a diffuse peak is observed in the region 21° for micro- and hollow powders of silicon dioxide, which indicates the amorphous phase of SiO_2 (Fig. 4b). Peaks indicating the presence of crystalline phases of silicon dioxide are absent.

It follows from the diffuse reflection spectra (Fig.5) that the spectral reflectance in the UV and visible regions reaches 90% for micro- and hollow powders of ZnO and TiO_2. The reflectivity of the micropowder is higher than that of hollow powders in the wavelength region from the edge of the main absorption to the near IR region. The smaller value of the spectral reflectance of hollow powders is due to the high concentration of intrinsic defects in the crystal lattice of nanostructured particles relative to the microparticles. At the same time, there is a competing process of increasing the reflectance by nanoparticles, associated with the scattering of light by small particles. In the near-IR region, the reflection coefficient of hollow powders is significantly reduced in comparison with micropowders. The difference in ρ values reaches 15-40%, which is determined by the high concentration of free charge carriers and chemisorbed gases absorbing in this spectral region [9]. The effect of decreasing the reflectance in the near-IR region is typical for hollow SiO_2 particles, whereas for microparticles there is no absorption in this region. Reflectance values for hollow particles in the region above 400 nm are 5% greater than in micropowders. In the UV region, a "dip" is recorded for the hollow particles - a decrease in the values of ρ to 40%.

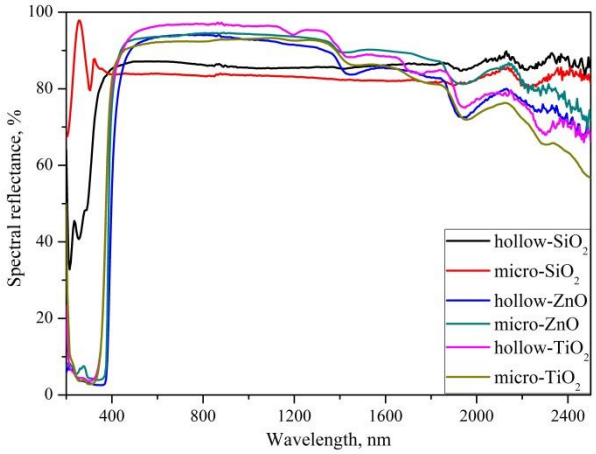

Fig.5 Diffuse reflectance spectra of hollow and microparticles of ZnO, TiO_2, SiO_2.

The reflectance of coatings based on micropowders and hollow particles of TiO_2 and ZnO reaches 80% in the region from 400 to 1200 nm, in the near IR region it decreases to 35%. In this region, the absorption bands 1190, 1405, 1690, 1740, 1830, 1930, 2275, 2360, 2460 nm are also recorded, which are similar to the absorption bands of the binder, some of them coincide

with the absorption bands of micropowders. For coatings based on SiO_2 is typical decrease of the reflectance in the region from 400 to 1200 nm to 60%. Such low value of reflectance was not typical for powders for which a reflectance reached 95 % in the UV region.

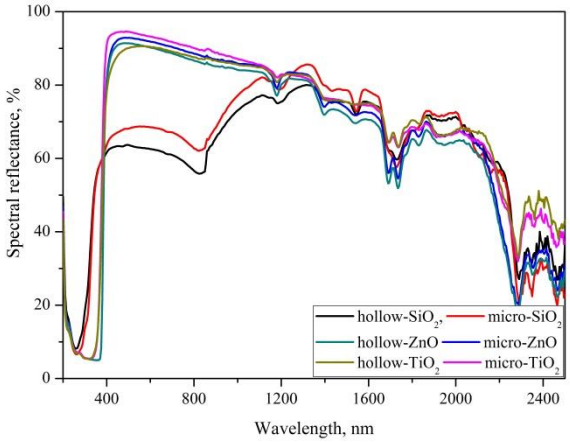

Fig.6 Diffuse reflectance spectra of coating based on hollow and microparticles of ZnO, TiO_2, SiO_2.

From the spectra of induced absorption after proton irradiation ($\Delta\rho_E = \rho_{E0} - \rho_{EF}$, where ρ_{E0} and ρ_{EF} are the spectra of diffuse reflection before and after irradiation, respectively) with an energy of 100 keV, fluence 5×10^{15} cm^{-2} (Fig. 7) powders of micro- and hollow particles it follows that the effect of ionizing radiation creates color centers whose bands form a continuous absorption spectrum in the UV and visible regions. ZnO powders are characterized by absorption bands with a high intensity in the range from 2 to 3.2 eV, in the near-IR region the intensity of the bands is insignificant. The high intensity bands have hollow particles of zinc oxide, the smallest – micropowders. The integral absorption band for hollow particles is shifted to the red region, the intensity of which closely coincides with the band for the microparticles.

After irradiation of TiO_2 powders, protons in the induced absorption spectra show absorption bands in the visible and near-IR regions. In the spectrum of micropowders, the intensity of the absorption bands in the short-wave region is larger than the intensity of the bands in the visible and near-IR regions. A distinctive feature of these spectra is that in the absorption spectra of powders from hollow particles there is practically no absorption in the near-IR region, while in the micropowder spectra it is not only recorded, but in absolute value, close to absorption in the UV region. In the spectra of induced absorption of silicon dioxide, well-separated absorption bands are recorded in the short-wavelength region. The lowest intensity of the bands is characteristic for hollow particles, the largest for microparticles. The bands intensity of SiO_2 nanoparticles is higher in comparison with the intensity of nanopowders ZnO and TiO_2.

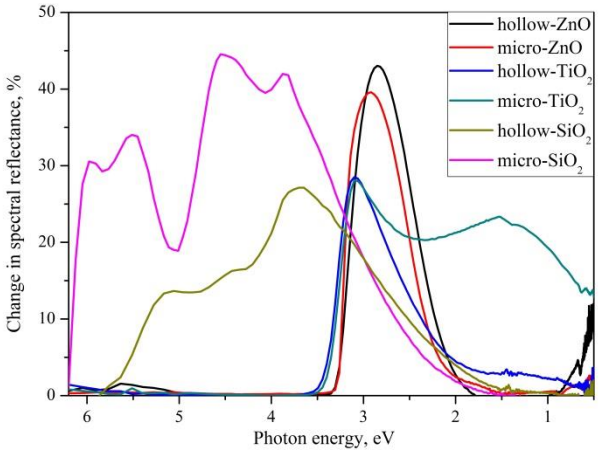

Fig.7 Change in spectral reflectance of hollow and microparticles of ZnO, TiO_2, SiO_2 after 100 keV proton irradiation with fluence 5×10^{15} cm^{-2}

From the analysis of the spectra $\Delta\rho_E$ of proton-irradiated zinc oxide powders with micron-sized grains, taking into account the known energy of the absorption bands of intrinsic defects, capable of absorbing in these ranges [10-15], it follows that the main contribution to the absorption is made by interstitial zinc ions $Zn_i^{\bullet}$, oxygen vacancies $V_O^{\bullet\bullet}$, zinc vacancies V_{Zn}' and V_{Zn}''. Nanopowders irradiated by protons have a similar spectrum of $\Delta\rho_E$ with micropowders, but the intensity of the bands in their spectra is higher. For both micro- and nanostructured particles, the absorption bands in the energy range from 1 to 2 eV have a low intensity. These bands are due to the interstitial oxygen O_i' and O_i^X and vacancies of oxygen V_O^X.

For titanium dioxide, the absorption in the UV region is determined by the defects of the cation sublattice, in the near-IR region by the defects of the anion sublattice [16-21]. After irradiation of the hollow particles, vacancies of the cation sublattice are formed to a lesser extent, which include vacancies V_{Ti}'''' and V_{Ti}'''. At room temperature, they correspond to absorption bands at 1.15 and 1.44 eV. This conclusion is typical not only for hollow particles of titanium dioxide powders, it is also valid for powders of this compound of micron sizes modified by nanoparticles of other compounds, as well as enriched in oxygen by various methods: treatment with tetro- and peroxoborates and peroxides, treatment with ultraviolet in oxygen and in the atmosphere [22]. In all these cases, a significantly lower intensity of the absorption bands by defects in the cation sublattice is recorded in comparison with the defect bands of the anion sublattice.

The energy position of the bands of radiation-induced absorption in the spectra of micro- and hollow powders of SiO_2 is the same or very close. In the high-energy region of the spectrum, a band is recorded at 5.96-6.02 due to the surface centers of E'_s [23-27] and the band at 5.46-5.48, determined either by vacancies in oxygen (E'_δ) or by oxygen vacancies , which captured hydrogen

atoms (E'_β). In the low-energy region of the spectra, the absorption bands at 4.45-4.5 are referred to the surface centers of E'_s.

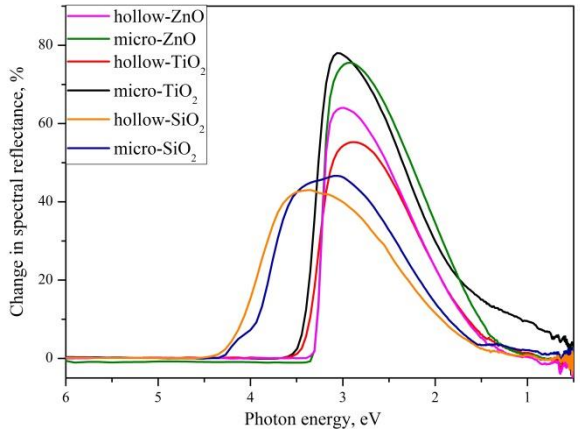

Fig.7 Change in spectral reflectance of coatings based on hollow and microparticles of ZnO, TiO_2, SiO_2 after 100 keV proton irradiation with fluence 5×10^{15} cm^{-2}

In the absorption spectra of the coatings (Fig. 7), samples of coatings from micropowders TiO_2 have the highest absorption, the peak of which lies in the visible region of 3.08 eV, which coincides with the value of the pigment. For hollow particles, the position of the peak absorption is close to 2.7 eV. The high absorption in coatings based on TiO_2 microspheres has a value in the peak near 55%. It follows from this that the degradation of optical properties of coatings from TiO_2 microspheres is smaller in comparison with coatings from micropowders TiO_2. A similar pattern is observed for coatings based on hollow and microparticles ZnO, a high intensity of the integral band for coatings from microparticles, which reaches 75%, but a lower intensity of the integral band for coatings based on hollow particles, which values are 63%. At the same time, we observed a different situation in describing the degradation of optical properties for which zinc oxide powders irradiated by protons, where the concentration of radiation defects causing the integral absorption band was higher for hollow ZnO particles. Degradation of coatings based on hollow SiO_2 particles under the action of 100 keV protons also occurs less intensively than coatings based on SiO_2 microparticles. Moreover, the intensity of the integral band has the smallest values (42%) of the investigated coatings based on ZnO and TiO_2. It should be noted that this band is somewhat tightened in the UV region of the spectrum and width at half-height low than the integral band of coatings based on ZnO.

From the physical point of view, it is also convenient to estimate the optical properties from the solar absorptance since the absorption bands of the defects in ZnO, TiO_2 and SiO_2 powders are located in different regions of the spectrum. Whereas the radiation stability is conveniently estimated from the change in the solar absorptance ($\Delta\alpha_s$).

After calculating the solar absorptance it follows (Table 2) that the smallest value of α_s has microcrystal-TiO_2 coatings. Whereas microspheres based coating shows high optical properties for ZnO. Exposure of the proton irradiation leads to degradation of coatings. It is established that the use of hollow particles leads to an increase in the radiation stability of coatings for all types of particles. The smallest degradation in coatings based on SiO_2 microspheres, but the initial optical properties are not so high. The best combination of the initial optical properties and their radiation stability to the impact of accelerated protons is typically for coatings based on ZnO microspheres. Thus, the efficiency of the SiO_2, TiO_2 and ZnO microspheres particle pigment compare with microcrystal particle pigment are 8 %, 32 % and 36 %, respectively.

Table 2. The values of α_s before irradiation and $\Delta\alpha_s$ after 100 keV proton irradiation of coatings based on the TiO_2, ZnO and SiO_2 microcrystal and microsphere particles.

Coating	α_s	$\Delta\alpha_s$
microcrystal-TiO_2	0.175±0.012	0.268±0.023
microsphere-TiO_2	0.214±0.017	0.203±0.031
microcrystal-ZnO	0.180±0.011	0.241±0.026
microsphere-ZnO	0.203±0.011	0.177±0.024
microcrystal-SiO_2	0.274±0.025	0.132±0.052
microsphere-SiO_2	0.325±0.032	**0.121±0.062**

4 DISCUSSION

Defect formation under proton irradiation of oxide powders is caused by radiation damage, which is determined by at least two processes. The first is the ionization mechanism that is characteristic of the surface layer, when a proton with high energy strikes an interatomic bond, destroys it, captures an electron and forms two ionized atoms:

$Me_{Me}^{X} + O_O^{X} + (H^{\bullet})^* \rightarrow (Me_{Me}^{X})^* + (O_O^{X})^* + H^{\bullet}$,

where Me_{Me}^{X}, O_O^{X} – atoms of cations and oxygen at lattice sites; $(H^{\bullet})^*$, $H^{\bullet}$ – accelerated and thermolysed proton.

On the surface, random processes of knocking out weakly bound oxygen with the formation of anion vacancies are also possible. In this case, the proton also captures the electron. The knocked out oxygen produces secondary atomic collisions. The second process of primary radiation damage, along with the first one, occurs in the volume of the polycrystal. It is carried out mainly by knocking out atoms from the nodes with the formation of vacancies by the following reactions:

$Me_{Me}^{X} + O_O^{X} + (H^{\bullet})^* \rightarrow V_{Me}^{\prime\prime} + Me_i^{\bullet\bullet} + O_O^{X} + H^{\bullet} \leftrightarrow V_{Me}^{\prime} + Me_i^{\bullet\bullet} + O_O^{X} + H$

$V_{Zn}^{\prime} + Me_i^{\bullet\bullet} \leftrightarrow V_{Me}^{X} + Me_i^{\bullet}$

$Me_{Me}^{X} + O_O^{X} + (H^{\bullet})^* \rightarrow Me_{Me}^{X} + V_O^{\bullet\bullet} + O_i^{\prime\prime} + H^{\bullet} \leftrightarrow Me_{Me}^{X} + V_O^{\bullet\bullet} + O_i^{\prime} + H$

$V_O^{\cdot\cdot} + O_i' \leftrightarrow V_O^{\cdot} + O_i^X$.

Thermalized hydrogen and oxygen can diffuse from the lattice to the surface of the polycrystal, followed by desorption. The defects remaining after this stage are in equilibrium and can be kept for a long time. These defects will determine the optical properties of the irradiated powder. Thermalized protons can interact with zinc vacancies or interstitial oxygen and form stable defects (V_{Me}-H) [28].

The products of the destruction of silicone varnish are cyclic oligomers - from the trimer to the heptadecamer. The common mechanism of their formation assumes the emergence of cyclic intermediate structures with the participation of the terminal group, in which the coordinated rupture and bonding occurs [29, 30]:

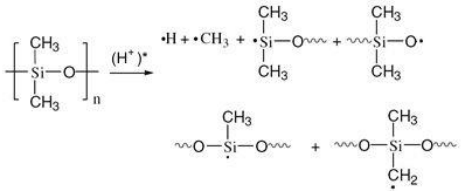

The increased radiation stability to the action of protons of hollow particles in comparison with microparticles is probably due to the fact that in these particles the probability of radiation defects formation in the volume of spherical particles is small because of the absence of material inside the hollow particle. Such structures also have small ionization losses and a high ability to relax radiation defects in a thin layer of the sphere. The high radiation stability of hollow SiO_2 particles can be attributed to the presence of an amorphous structure, where the intrinsic and radiation defects can be reflected in such an unordered structure and restored more quickly.

Improving the radiation stability of coatings based on hollow particles can be due to the formation of metal-organic complexes between the polymers of silicone varnish and inorganic compounds of oxide powders upon irradiation. Under such conditions, the polymer radicals induced by ionizing radiation crosslinked on the developed surface of the hollow particles.

CONCLUSION

In summary, the initial α_S of the coatings based on micropowders is higher than that for the microsphere based coatings. It is found that the radiation stability under proton exposure (100 keV, $5x10^{15}$ cm^{-2}) of the microspheres based coatings is higher than for the micropowders based coatings. This effect associated with the relaxation defects on high specific surface area of the hollow particles and the low ionization losses therein. Evaluation of other parameters for use such pigments in thermal control coatings will be continued.

REFERENCES

1. Tribble A.C., Lukins R., Watts E., Borisov V.A., Demidov S.A., Denisenko V.A., Gorodetskiy A.A., Grishin V.K., Nauma S.F., Sergeev V.K., Sokolova S. P. United States and Russian Thermal Control Coating Results in Low Earth Orbit. *Journal of Spacecraft and Rockets*, 33(1):160-166, 1996.
2. Mikhailov M.M., Neshchimenko V.V., Yuryev S.A. Optical properties and radiation stability of submicro- and nanopowders titanium dioxide measured in situ. *Radiation Physics and Chemistry*, 121:10-15, 2016.
3. Blondiaux G., Valladon M., Ishii K., Debrun J. L. Search for the influence of chemical effect on the stopping power: the case of oxides, *Nucl. Inst. Methods*, 168: 29-31, 1980.
4. Neshchimenko V. V., Li Chundong, Mikhailov M. M.. Radiation stability of TiO_2 hollow particles pigments and coatings synthesis by hydrothermal methods from TTIP, *Dyes and Pigments*, 145: 354-358, 2017.
5. Xiong Wen (David) Lou, Lynden A. Archer, Zichao Yang. Hollow Micro - Nanostructures: Synthesis and Applications, *Advanced Materials*, 20(21): 3987-4019, 2008.
6. Kim Y.J., Chai S.Y., Lee W.I. Control of TiO_2 structures from robust hollow microspheres to highly dispersible nanoparticles in a tetrabutylammonium hydroxide solution. *Langmuir*, 23: 9567-9571, 2007.
7. Yan C., Xue D., Polyhedral construction of hollow ZnO microspheres by CO_2 bubble templates. *J. Alloy. Compd*. 431, 241–245, 2007.
8. Ziwei Deng, Min Chen, Shuxue Zhou, Limin Wu A Novel Method for the Fabrication of Monodisperse Hollow Silica Spheres, *Langmuir* 22(14):6403-7, 2006.
9. D.A. Burns, E.W. Ciurczak (Eds.), Handbook of Near-Infrared Analysis, second ed., Marcel Dekker, New York, 2001, p. 814.
10. Lin B., Fu Z., Jia Y., Green Luminescent Center in Undoped Zinc Oxide Films Deposited on Silicon. *Appl. Phys. Lett.*, 79, 943, 2001.
11. Xu P.S., Sun Y.M., Shi C.S., Xu F.Q., Pan H.B., The electronic structure and spectral properties of ZnO and its defects, *Nucl. Instr. Meth. Phys. Res. B.*, 199, 286–290, 2003.
12. Oba F., Togo A., Tanaka I., Paier J., Kresse G., Defect energetics in ZnO: A hybrid Hartree-Fock density functional study, *Phys. Rev. B.*, 77, 245202(1–6), 2008.
13. Hu J., Pan B.C. J., Electronic structures of defects in ZnO: hybrid density functional studies, *Chem. Phys*., 129, 154706(1-8), 2008.
14. Sun Y., Wang H., The electronic properties of native interstitials in ZnO, *Physica B.*, 325, 157-163, 2003
15. Erhart P., Albe K., Klein A., First-principles study of intrinsic point defects in ZnO: role of band

structure, volume relaxation, and finite-size effects, *Phys. Rev. B.*, 73, 205203(1–9), 2006.
16. Nowotny J. Titanium dioxide-based semiconductors for solar-driven environmentally friendly applications: impact of point defects on performance, *Energy Environ. Sci.* 1, 565-572, 2008.
17. He J., Behera R.K., Finnis M.W., Li X., Dickey E.C., Phillpot S.R., Sinnott S.B. Prediction of high-temperature point defect formation in TiO_2 from combined ab initio and thermodynamic calculations, *ActaMaterialia*, 55, 4325-4337, 2007..
18. Chena J., Linb L.-B., Jinga F.-Q. Theoretical study of F-type color center in rutile TiO_2, J*ournal of Physics and Chemistry of Solids*, 62, 1257-1262, 2001.
19. Seebauer E.G., Kratzer M.C. Charged point defects in semiconductors, *Materials Science and Engineering R*, 55, 57-149, 2006.
20. Nakamura I., Negishi N., Kutsuna S., Ihara T., Sugihara S., Takeuchi K. Role of oxygen vacancy in the plasma-treated TiO_2 photocatalyst with visible light activity for NO removal . *Journal of Molecular Catalysis A: Chemical*, 161, 205-212, 2000.
21. Kuznetsov V.N., Serpone N. On the origin of the spectral bands in the visible absorption spectra of visible-light-active TiO_2 specimens. Analysis and assignments. *J. Phys.Chem. C*, 113, 15110-15123, 2009.
22. Mikhailov M.M., Sokolovskii A.N. Photostability of Coatings Based on TiO_2 (Rutile) Doped with Potassium Peroxoborate. *Journal of Spacecrafts and Rockets*, 43, 451-455, 2006.
23. Li C., Mikhailov M.M., Neshchimenko V.V. Radiation stability of SiO_2 micro- and nanopowders under electron and proton exposure, *Nucl. Instr. and Meth. B*, 319, 123-127, 2014.
24. Zatsepina A. F., Kortova V.S., Biryukova D.Y. Electron-emission activity of defects in surface layers of crystalline and vitreous silica, *Radiation Effects and Defects in Solids*, 157, 595-601, 2002.
25. Boscaino R., Cannas M., Gelardi F.M., Leone M. ESR and PL centers induced by gamma rays in silica // *Nucl. Instr. and Meth. B*, 116, 373-377, 1996.
26. Skuja L. Optically active oxygen-deficiency-related centers in amorphous silicon dioxide, *Journal of Non-Crystalline Solids*, 239, 16-48, 1998.
27. Vaccaro L., Morana A., Radzig V., Cannas M. Bright Visible Luminescence in Silica Nanoparticles, *J. Phys. Chem. C*, 115, 19476–19481, 2011.
28. Brauer G., Anwand W., Grambole D., Grenzer J., Skorupa W., Čížek J., Kuriplach J., Procházka I., Ling C.C., So C.K., Schulz D., Klimm D., Identification of Zn-vacancy–hydrogen complexes in ZnO single crystals: A challenge to positron annihilation spectroscopy, *Phys. Rev. B*., 79, 115212(1-15), 2009.
29. Haiying Xiao, Chundong Li, Dezhuang Yang, Shiyu He. Optical degradation of silicone in ZnO/silicone white paint irradiated by <200 keV protons. *Nucl. Instr. and Meth. B.*, 266, 3375-3380, 2008.
30. Mingwei Di, Shiyu He, Ruiqi Li, Dezhuang Yang. Radiation effect of 150 keV protons on methyl silicone rubber reinforced with MQ silicone resin. *Nucl. Instr. and Meth. B.*, 248, 31-36, 2006.